Knife-Edge Scanning Microscopy for Connectomics Research

Yoonsuck Choe, David Mayerich, Jaerock Kwon, Daniel E. Miller, Ji Ryang Chung,
Chul Sung, John Keyser, and Louise C. Abbott

Abstract

In this paper, we will review a novel microscopy modality called Knife-Edge Scanning Microscopy (KESM) that we have developed over the past twelve years (since 1999) and discuss its relevance to connectomics and neural networks research. The operational principle of KESM is to simultaneously section and image small animal brains embedded in hard polymer resin so that a near-isotropic, sub-micrometer voxel size of 0.6 μm × 0.7 μm × 1.0 μm can be achieved over ∼1 cm^3 volume of tissue which is enough to hold an entire mouse brain. At this resolution, morphological details such as dendrites, dendritic spines, and axons are visible (for sparse stains like Golgi). KESM has been successfully used to scan whole mouse brains stained in Golgi (neuronal morphology), Nissl (somata), and India ink (vasculature), providing unprecedented insights into the system-level architectural layout of microstructures within the mouse brain. In this paper, we will present whole-brain-scale data sets from KESM and discuss challenges and opportunities posed to connectomics and neural networks research by such detailed yet system-level data.

I. Introduction

In the past few years, a new term *connectomics* emerged in neuroscience. Connectomics is the study of connectomes, where connectome means the full connection matrix of the brain [1]. The basic idea behind connectomics is that by knowing the full architectural circuit diagram of the brain, we can start understanding the function of the brain. One can even say that brain function is largely determined by how it is wired (to quote Sebastian Seung [MIT] during his TED talk, "I am my connectome").

This surge of interest in connectomics has been enabled by a confluence of multiple technological advances including high-performance computing, Diffusion MRI (magnetic resonance imaging), and a number of new physical sectioning microscopy techniques (see [2], [3] for an extensive review).

Choe, Miller, Chung, Sung, and Keyser are with the Department of Computer Science and Engineering, Texas A&M University. Abbott is with the Department of Veterinary Integrative Biosciences, Texas A&M University. Mayerich is with the Beckman Institute for Advanced Science and Technology, University of Illinois, Urbana-Champaign. Kwon is with the Department of Electrical and Computer Engineering, Kettering University. Correspondences should be directed to Yoonsuck Choe (choe@tamu.edu).

This project was funded by NIH/NINDS (#1R01-NS54252), NSF (#0905041,#0079874), the Texas Advanced Technology Program (#ATP-000512-0146-2001, #ATP-000512-0261-2001), and 3Scan. 3D volume rendering was done with MeVisLab.

Diffusion MRI is based on magnetic resonance imaging of water molecule movement (diffusion) patterns that are restricted by neural tracts to infer fiber direction (see [4], [5] for a review). Diffusion MRI has been used successfully to map large-scale inter-area neural tracts in large animal brains such as the human brain, however, the voxel resolution is on the order of several hundred μms (e.g., a high-resolution approach gives 156 μm in-plane resolution [6]), thus detailed circuits based on individual fibers cannot be reconstructed.

Major advances have been made on the microscopy side, with high-volume, high-resolution methods that employ physical sectioning, as opposed to optical sectioning (see [3] for a review). 3D volume imaging in microscopy has been dominated by optical sectioning methods such as confocal microscopy or two- or multi-photon imaging [7], [8], [9]. However, these approaches can only image as deep as several hundred micrometers since beyond that point the signal-to-noise ratio becomes too high. Furthermore, the point spread function in the z-direction (depth direction) is significantly worse than x and y, thus details can be lost in the z direction. An emerging alternative to optical sectioning is physical sectioning. These approaches include Knife-Edge Scanning Microscopy (KESM) [10], [11], [3], [12] (cf. [13] that adopted the same principles as KESM), Array Tomography [14], and All-Optical Histology [15] that use light microscopy (LM) or fluorescence imaging (see [16] for a general overview of LM), while Serial Block-Face Scanning Electron Microscopy (SBF-SEM) [17], Automatic Tape-Collecting Lathe Ultramicrotome (ATLUM) [18], and Focused Ion Beam Scanning Electron Microscopy (FIB/SEM) [19] utilize electron microscopy (EM) for the actual imaging. Note that Array Tomography also supports electron microscopy. The typical linear dimension of the imaged volume is on the order of 1 cm for LM and 100 μm for EM. Note that ATLUM can potentially section much larger volumes quickly, but subsequent EM imaging time is a major bottleneck. The respective voxel size (linear dimension) is on the order of 0.5 μm (LM) and 10 nm (EM). These high-volume, high-resolution microscopy techniques enable the imaging of neural circuits in whole small animal brains such as that of the mouse. This kind of data can give us unprecedented insights into the wiring of the brain, and in turn the function of the brain.

In this paper, we will first give a brief overview of KESM, and then showcase our whole-brain-scale data at sub-micrometer resolution, obtained from the C57BL/6 mouse. We will then present how our data can be utilized in connectomics (and computational neuroscience) research,

and discuss current limitations and future directions of the burgeoning field of connectomics.

II. Knife-Edge Scanning Microscopy

Fig. 1 shows a photo of the KESM with its major components: (1) high-speed line-scan camera, (2) microscope objective, (3) diamond knife assembly and light collimator, (4) specimen tank (for water immersion imaging), (5) three-axis precision air-bearing stage, (6) white-light microscope illuminator, (7) water pump (in the back) for the removal of sectioned tissue, (8) PC server for stage control and image acquisition, (9) granite base, and (10) granite bridge. See [10], [20] for technical details.

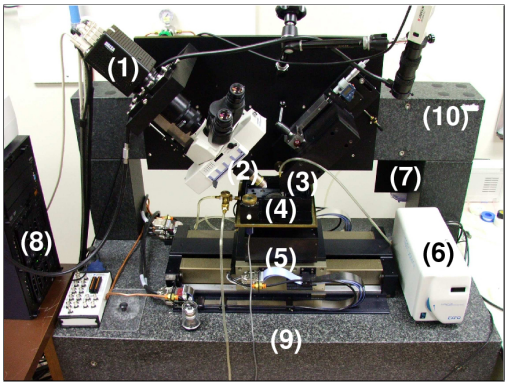

Fig. 1. **The Knife-Edge Scanning Microscope (KESM).** Adapted from [10], [3].

The imaging principle of KESM is shown in Fig. 2. The objective and the knife is held in place, while the specimen affixed on the positioning stage moves, and gets scraped against the diamond knife, generating a thin section flowing over the knife. Line-scan imaging is done near the very tip of the knife where the distortion is minimal. Illumination is provided through the diamond knife (green beam indicates the light path).

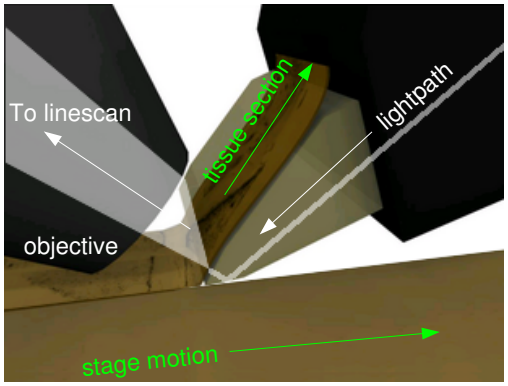

Fig. 2. **Tissue Sectioning and Imaging in KESM.** Adapted from [10], [3].

In the above configuration, KESM performs transmission imaging, However, a beam-splitter is installed in the optic train (Fig. 1(2)) so that reflective imaging is also possible [11] (note: [13] employs this configuration). In this case, the light path comes from the back of the granite bridge, through a hole bored through the bridge. The beam splitter can also hold excitation filters for fluorescence imaging.

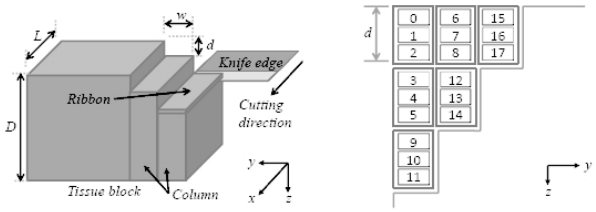

Fig. 3. **Lateral Sectioning.** Adapted from [21].

Due to the limited field of view of the microscope objective and the width of the knife, the whole block face (typically 1 cm^2) cannot be scanned in one sweep. We use a lateral sectioning approach to overcome this limitation (Fig. 3). In the figure, L is the length, D is the height of the specimen block, w is the cutting width (tissue section width), and d is the depth of one plank. Each plank is a collection of multiple tissue sections (numbered 0 to 17 to the right: the thickness of the tissue section is exaggerated). The cutting proceeds in the numbered order. Typically, each plank consists of 10 to 20 images (10 µm to 20 µm in thickness). With about 10 lateral columns, the maximum difference in the shallowest and the deepest part of the exposed tissue block is 100 µm to 200 µm. The boundaries between vertical columns are torn rather than cut, but the damage in this region is usually $<\sim$5 µm wide. Please refer to [22], [21] where we discuss these issues in detail. An in-house custom control software is used to coordinate the lateral sectioning and imaging process [21]. Imaging time for a 1 cm^3 cube at 0.6 µm $\times$ 0.7 µm $\times$ 1.0 µm is $\sim$100 hours.

III. KESM Mouse Brain Data

Using KESM, we have been able to obtain whole-brain-scale data from the mouse. Our earliest data were from Golgi-stained (neuronal morphology) and India ink-stained (vasculature) mouse brains. These scans were completed in 2008, and subsequently reported in [24], [23]. Due to a frame buffer limit, the top 1/3 of the anterior part of the Golgi brain was not imaged, although the entire brain was sectioned. On the other hand, the India ink data set spanned the whole brain. In early 2010, we also scanned a whole mouse brain stained with Nissl, to reveal the cell body distribution across the entire mouse brain [25]. A full Golgi brain was imaged later in 2010 (data not published yet). In all cases, the voxel resolution was 0.6 µm $\times$ 0.7 µm $\times$ 1.0 µm.

Fig. 4 shows KESM data from a Golgi-stained mouse brain (horizontal sections). Each plate is an overlay of 20 images (each image is 1 µm thin), taken at an interval of 3 sections thus representing a 60 µm-thick tissue block. A web-based rendering approach was used for the visualization [26], which utilizes the Google Maps API for layering multiple images.

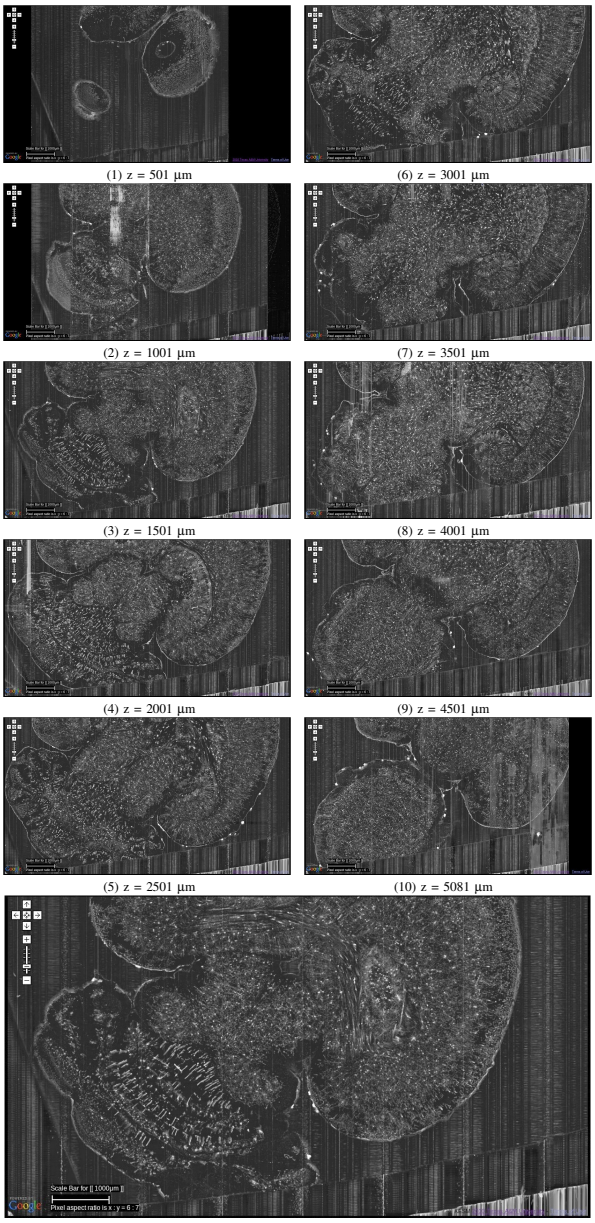

Fig. 4. **KESM Golgi Data Set (Horizontal Sections).** A different visualization of data set acquired in 2008 and previously reported in [23], [24] is shown. Each image is an overlay of 20 images (each 1 µm thin) at an interval of 3 sections (60 µm-thick volume). Scale bar = 1mm. Voxel size = 0.6 µm × 0.7 µm × 1.0 µm. (Images were inverted for easier view.)

The upper right corner is anterior, and the lower left corner is posterior. Each image is made up of nine lateral columns, and consists of an overlay of twenty 1 µm-thick sections. The number below each image shows the depth within the data volume. These are data acquired in 2008, and reported in [24], [23]. To our knowledge, this is the first data set of its kind: mouse brain Golgi data at the whole brain scale, at sub-micrometer resolution. Our techniques have been adopted and validated by other labs to produce similar results at a slightly higher resolution of 0.33 µm × 0.33 µm × 1.0 µm/voxel [13].

Each image in the 3D image stack is 1 µm thin. A single image (a very small part of it) would look like Fig. 5*a*, so it is hard to get any insight about neuronal morphology or circuitry by going through such individual images one at a time. We found that overlaying several images helps reveal the intricate details of neuronal circuits (Fig. 5*b–c*, Fig. 6).

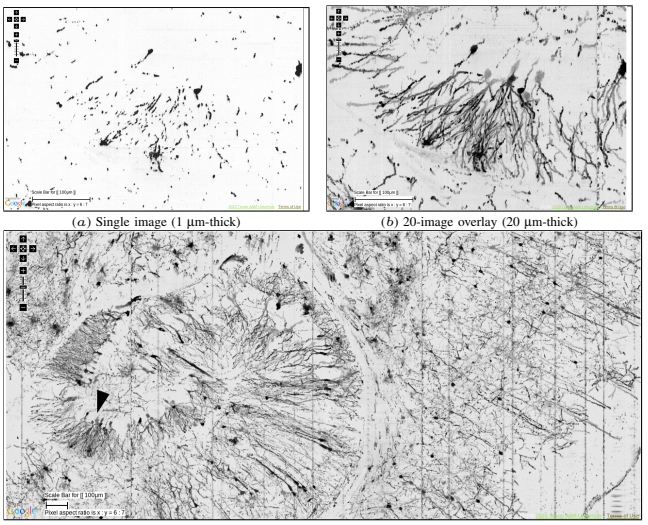

Fig. 5. **KESM Golgi Data (Hippocampus).** Different visualization of data set previously reported in [24], [23]. (*a*) is a single image, and (*b*) is an overlay of 20 images (with depth attenuation) from the same region as in (*a*). This is part of the dentate gyrus in the hippocampus. (*c*) The curved structure of the dentate gyrus is more prominently visible in this zoomed-out view (overlay of 20 images at an interval of 3 sections = 60 µm-thick volume). The arrowhead marks where (*a*) and (*b*) are located. Scale bar = 100 µm.

Fig. 6 shows a close-up view of the visual cortex from the same Golgi data set, using minimum intensity projection (MIP). Again, the image shown is an overlay of 200 successive sections (total thickness = 200 µm). At this resolution, fine details like dendritic spines can be observed. Several pyramidal cells (upper left) and their apical dendrites (diagonally stretching toward the lower right), and a couple of spiny stellate cells can be seen (upper right).

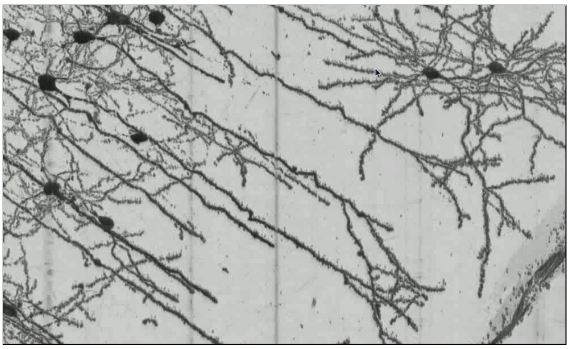

Fig. 6. **KESM Golgi Data (Cortex).** Minimum intensity projection of a stack of 20 images is shown. From data previously reported in [23].

IV. 3D Aspect of the KESM Data

With visualizations like Fig. 4–6, it is easy to neglect the fact that KESM data sets are fundamentally 3D. With a voxel resolution of a near-isotropic 0.6 µm × 0.7 µm × 1.0 µm, a full 3D exploration and analysis is possible. In this section, we present some 3D visualizations of the KESM data sets to emphasize the above point.

Fig. 7 shows a tiny subset of the same Golgi data set presented above. The raw data are basically an image stack that looks like Fig. 7a. Simple thresholding gives Fig. 7b, revealing the intricate structure within the data volume.

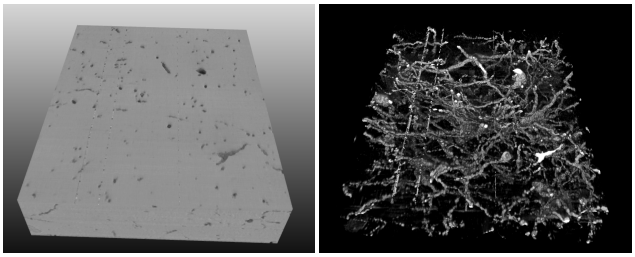

(a) (b)

Fig. 7. **3D Aspect of KESM Data (Golgi).** Data block width = 360 µm, height = 80 µm.

Fig. 8 also shows the 3D-nature of the KESM data set. In this figure, cerebellar Purkinje cells are shows, with their planar dendritic trees. Again, the data volume shown can be explored in full 3D. However, since the microstructures stained with Golgi are tiny (on the order of µm's) it is hard to see anything if zoomed out to view the whole brain. We will discuss visualization and analysis strategies to overcome this issue in Sec. IX.

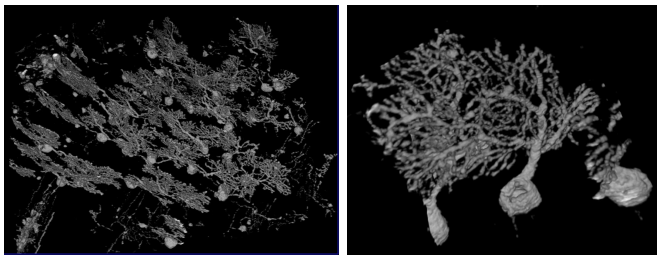

(a) (b)

Fig. 8. **KESM Golgi Data (Volume Visualization).** Volume visualization of cerebellar Purkinje cells is shown (using MeVisLab). Width (a) ∼ 500 µm, (b) ∼ 100 µm. Adapted from [23].

To appreciate the whole-brain scope of KESM data sets in 3D, we can look at the India ink data set that shows the full vascular network in the mouse brain. Although not directly involved in neural computation, the vascular network plays in important role in support of computation. Also, certain measures like BOLD (Blood-oxygen-level dependent) signals from fMRI (functional Magnetic Resonance Imaging) scans are used as an indicator of regional activity in the brain. Finally, the vascular network can also provide necessary scaffolding for neuronal migration. For example, [27] found that blood vessels in the olfactory bulb guide the migration of neuroblasts.

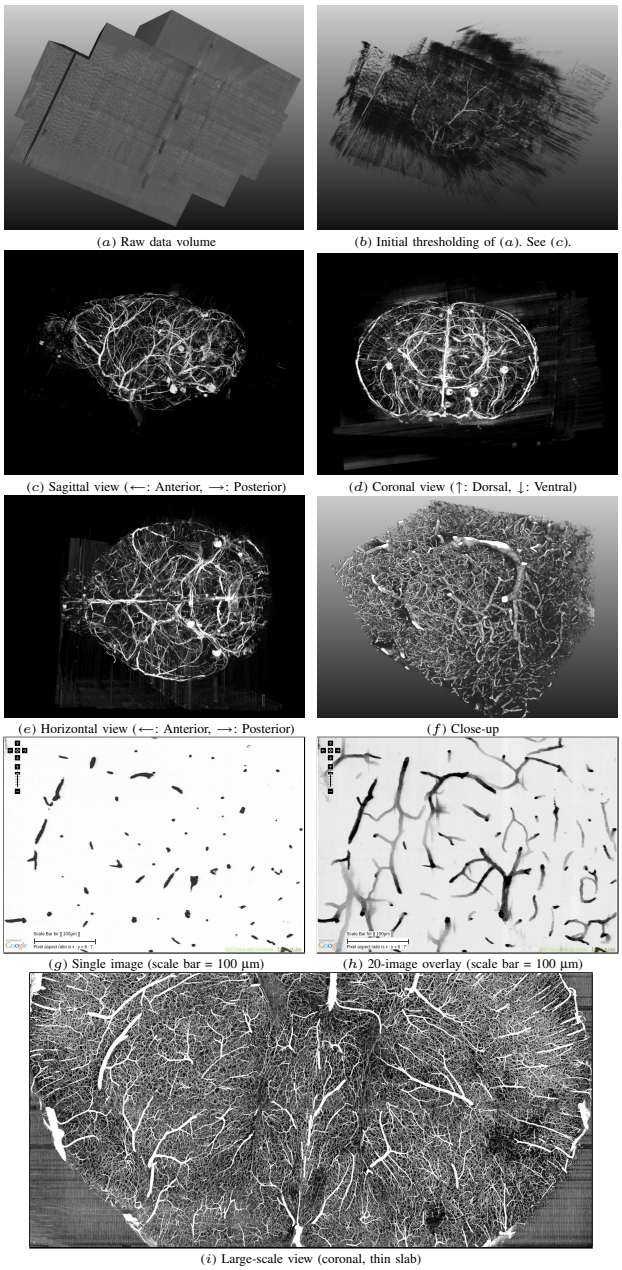

(a) Raw data volume

(b) Initial thresholding of (a). See (c).

(c) Sagittal view (←: Anterior, →: Posterior)

(d) Coronal view (↑: Dorsal, ↓: Ventral)

(e) Horizontal view (←: Anterior, →: Posterior)

(f) Close-up

(g) Single image (scale bar = 100 µm)

(h) 20-image overlay (scale bar = 100 µm)

(i) Large-scale view (coronal, thin slab)

Fig. 9. **KESM Vasculature Data.** Different visualization of data previously reported in [24], [23]. (c)–(e) adapted from [23] (scale bar = 100 µm). See text for details.

Fig. 9 presents various visualizations of the vascular network data set. The data set presented here was obtained in 2008, and reported in [24], [23]. In Fig. 9, (a) shows the raw data block in a sagittal view. (b) shows a lightly thresholded version of (a) so that the boundary of the raw data block and the content within can be seen at the same time. (c) is a fully thresholded version of (a) and (b). (d)–(e) show the coronal and horizontal views, respectively. We can clearly see the shape of the brain, thanks to the thick blood vessels that are distributed across the entire brain. (f) shows the intricate details within an 1.5 mm-wide block. (g) shows a single image, and (h) an overlay of 20 images (depth attenuation). (i) shows a large-scale view of a thin slab (coronal section).

V. Exploring the 3D Golgi Data

Unlike the vascular network data, Golgi data are hard to visualize at the whole-brain scale. Figs. 10*a*–*b* show this difficulty, where a 2.88 mm-wide block from [24], [23] is shown. In this view, most of the thin fibrous structures are washed out. To observe the local circuits, we need to view a thin slab at a time. As shown in Fig. 10*c*–*e*, a sweep through the depth of the block (perpendicular to the screen, away from the reader) from Fig. 10*b* can reveal intricate circuits across a large region in the brain. Since the data block is fully 3D, this kind of sweep can be done in any direction, as shown in Fig. 10*f*, which shows a sagittal view. Furthermore, instead of going in a one-directional sweep, the sweep direction can be dynamically adjusted to inspect a specific region of interest. Other approaches for visualizing densely packed fibers like this are also emerging [28].

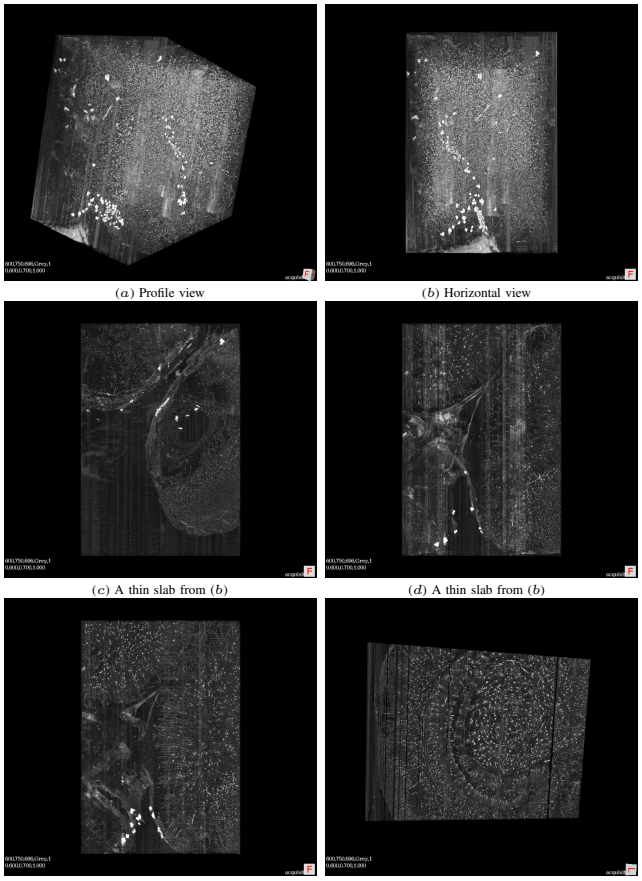

(*a*) Profile view (*b*) Horizontal view

(*c*) A thin slab from (*b*) (*d*) A thin slab from (*b*)

(*e*) A thin slab from (*b*) (*f*) A thin slab from sagittal section of (*b*)

Fig. 10. **3D View of the KESM Golgi Data Set.** KESM Golgi data from [23], [24]. Block width = 2.88 mm.

VI. From Raw Data to Structure: Reconstruction

Once the volume data are obtained, the next step is to extract the complete geometric structure from the raw data. Fig. 11 summarizes this process, called reconstruction.

The image forming process can be summarized as $g \circ f$, a composition of g and f. On the other hand, the task of recovering the structural descriptions from the image data is basically the inverse: $\hat{f}^{-1} \circ \hat{g}^{-1}$, a composition of the segmentation ($\hat{g}^{-1}$) and the 3D reconstruction process ($\hat{f}^{-1}$). (The "$\hat{}$" symbol indicates that these functions are estimates.)

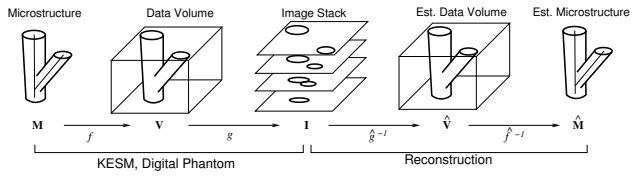

Fig. 11. **Microstructure-to-image Mapping and Reconstruction.**

Reconstruction is one of the major initial challenges in connectomics, with no existing solution yet in view. Current approaches for reconstruction include [29], [30], [31], [32], [33], [34], [35], [36], [37] (these include methods for EM as well as LM data). There are tools for manual reconstruction as well [38], and commercial packages [39], [40]. Neural-network-based approaches are also being explored [41], [42].

There are two main issues with reconstruction: (1) accuracy, and (2) computational demand. Typical accuracy of current approaches is around 95% (see e.g., [41]), which is not sufficient enough. Furthermore, even among human experts, there can be variation [43]. Computational demand is also high. For example, tracing a 128 $\times$ 128 $\times$ 128 voxel cube may take $\sim$ 200 seconds (on a Pentium 4, 2.4GHz processor) [44]. Considering that KESM data size is typically about 2 TB per brain, a simple calculation gives 2207 days, or just over 6 years. Compare that to the $\sim$100-hour KESM scanning time for a single mouse brain. (For EM, assuming a conservative voxel size of 30 nm $\times$ 30 nm $\times$ 30 nm, compared to the KESM voxel size of 0.6 µm $\times$ 0.7 µm $\times$ 1.0 µm, we get 15,556$\times$6 years on a single-CPU machine [note that this is based on a simplistic calculation: using a detailed reconstruction algorithm custom-made for EM data may take even longer].) Currently, the only fully reconstructed connectome is that of the nematode *C. elegans* [45], a small worm the size of $\sim$1 mm.

VII. From Structure to Function

Once the connectome is reconstructed, where do we go from there? We need to infer the function from the structure. This is not a trivial task, and there can be several dramatically different approaches.

Graph theoretical analysis: With a full connectivity matrix, we can use standard graph theoretic measures such as in-degree, out-degree, clustering index, etc. [46], [47], [48] and look for motifs [49].

Basic circuit analysis: Stereotypical patterns of local circuits are a hallmark of brain architecture. These patterns are called basic circuits, and using these as a building block, large-scale circuit analysis can be conducted [50].

Dynamic analysis: Certain dynamic parameters such as conduction delay can be estimated based on axon length and diameter. Simply calculating the delay distribution can already provide great insights into brain function. For example, [51] showed that the complexity of network dynamics critically depends on the delay distribution. Also see [52] on the relationship between neuroanatomy and brain dynamics.

Connectivity estimation: Data based on LM typically show only a fraction ($\sim$ 1% for Golgi) of the entire population of neurons. That is, the data is sparse. In this case, we need to estimate connectivity. Methods like those proposed by [53] can be used for this purpose. Also, a systematic simulation study can be conducted with a full synthetic circuit, by dropping a certain proportion of connections and observing the resulting change in behavior. The degree of redundancy in the connections (both for real and synthetic circuits) will play an important role here.

Linking with gene expression data: The connectome is fundamentally a static structure. How can the physiological properties be inferred from just the structure? [54] shows a possibly powerful solution to this: Use gene expression data. They found that gene expression and electrophysiological properties are closely correlated. The availability of very large gene expression atlases such as the Allen Brain Atlas [55] (22,000 genes), and imaging modalities such as Array Tomography that support molecular as well as EM imaging [14] are great resources for this kind of approach (see, e.g., [56]).

Inter- and intra-specimen variability estimation: Simply measuring the morphological variability among the same class of neurons can provide valuable insights into how redundant or specialized the functions are (Gerald Edelman, personal communication, 2009; see [57] for an existing morphological database). Even when connectivity is not known, just examining the dendritic trees can give deep insights into neural computation [58], [59].

Brute-force parameter search and simulation: Of course a straight-forward yet potentially valuable approach is to start with computational simulation based on detailed neuronal morphology (cf. the Blue Brain Project [56]). The reconstructed geometry can be used to construct multi-compartment models (see e.g. [60]). Appropriate parameters such as channel conductance, capacitance, etc. need to be figured out. Tools like NEURON, GENESIS, neuroConstruct, and NeuGEN can be used for multi-compartment simulation and parametrized synthetic circuit generation/simulation/analysis [61], [62], [63], [64], [65], [66], [67]. Data from the KESM can help narrow down on the range of various parameters for these simulations (see [68] for parameter constraining procedures).

Investigate the effect of link fidelity: A great matter of debate in connectomics is whether individual connections matter (detailed EM info needed), or whether they can be averaged (diffusion MRI is enough). Some results suggest that dropping even a single spike in the initial condition can have a global effect on the entire cortex within 0.5 second (see [69]'s large-scale simulation study of the thalamocortical system based on Diffusion Tensor Imaging data). However, considering that the brain in a normal operating environment is always anchored to the present input stimulus, constantly resetting the initial condition, this may not be a serious issue. Issues like these can be studied based on circuit data estimated from the KESM data sets.

Direct simulation on raw data: A rather far-fetched idea is to skip the reconstruction step and directly simulate based on the raw data (some image processing may be necessary to remove noise). The idea is simple: for each voxel, (1) assign a probability of excitation based on its gray-scale value, and (2) introduce a refractory period once activated. Each voxel will be initially off, and upon being stimulated, it will become active, and enter a short refractory period. The relative excitation dynamics can be weighted by linking to gene expression atlas data. A local activation rule will be used to activate adjacent regions, following the excitation probability assigned to each voxel. Due to the refractory period, activation can propagate with a directionality.

VIII. Discussion

The main contribution of the KESM is the ability to rapidly section and image large volumes of biological data at a submicrometer resolution. The main limitation is that it uses LM, so the resolution is diffraction limited. An associated problem is that dense stains cannot be used (such as those used for EM) so at present traditional histological stains like Golgi are used, which reveals only 1% of the entire neuronal population. Furthermore, Golgi does not stain thin axons very reliably. A combination of Golgi and tracers such as biocytin, or the use of fluorescence labeling will help address these issues.

KESM has the potential to open up connectomics research for small animal species other than the mouse. It does not need to be a vertebrate species either. We have done pilot scans of the octopus (*Octopus vulgaris*) brain (subesophageal mass and optic lobe) with encouraging results [70]. As these results suggest, the applicability of KESM is quite broad.

The kind of brain volume data generated by KESM and similar microscopy techniques can greatly benefit neural networks research. Neural networks can play an important role at multiple stages of connectomics research. First, neural networks can be used for tasks such as image processing, reconstruction, and cell detection (see, e.g., [41], [42]). Also, once a sufficiently large volume of circuitry data becomes available, the data can be used to (1) validate existing neural network models and theories, (2) construct anatomically correct neural network models for functional simulation, and/or (3) data-mine for principles of neural computation.

Finally, there are many open-ended questions. For example, is it possible that we can have a high-fidelity simulation

of the brain but cannot understand what is going on in the simulation? This is a possibility. Based on this, some even might argue that modeling and simulation does not give you any additional understanding about the phenomena that you are studying. However, we need to consider that simulations give us two important tools: (1) full access to the system state (read-out) and (2) full control over the system state (intervention). With a fully replicated simulation, we can conduct a full battery of experiments, and also have a unique opportunity to selectively damage or turn off parts of the system, which is an important requirement for inferring causality (see [71] for the importance of intervention). Another important question is about the role of theory in the analysis of connectomics data. Do we need good theory to make progress in connectomics research? A premature theory may only mislead, but theories based on broader perspectives, such as the importance of the sensorimotor loop [72], the role of time in neural networks [73], evolutionary perspective on brain function [74], etc. can help guide our exploration through the vast connectomics data.

IX. Conclusion

In this paper, we reviewed recent technological advances that enable connectomics research, and presented whole-brain-scale, submicrometer data from the Knife-Edge Scanning Microscope (KESM). Rich brain anatomy data from instruments like the KESM can open up many opportunities for neural networks research to advance our understanding of the central nervous system. We expect data like those from the KESM to help us rethink neural network models of the brain, and lead to major breakthroughs in emulating the brain function and behavior.

* For high-resolution images/videos visit http://kesm.org.

References

[1] O. Sporns, G. Tononi, and R. Kötter, "The human connectome: A structural description of the human brain," *PLoS Computational Biology*, vol. 1, p. e42, 2005.

[2] O. Sporns, *Networks of the Brain*. Cambridge, MA: MIT Press, 2011.

[3] Y. Choe, L. C. Abbott, D. Han, P.-S. Huang, J. Keyser, J. Kwon, D. Mayerich, Z. Melek, and B. H. McCormick, "Knife-edge scanning microscopy: High-throughput imaging and analysis of massive volumes of biological microstructures," in *High-Throughput Image Reconstruction and Analysis: Intelligent Microscopy Applications*, A. R. Rao and G. Cecchi, Eds. Boston, MA: Artech House, 2008, pp. 11–37.

[4] D. S. Tuch, T. G. Reese, M. R. Wiegell, and V. J. Wedeen, "Diffusion MRI of complex neural architecture," *Neuro*, vol. 40, pp. 885–895, 2003.

[5] P. J. Basser and D. K. Jones, "Diffusion-tensor MRI: Theory, experimental design and data analysis–A technical review," *NMR in Biomedicine*, vol. 15, pp. 456–467, 2002.

[6] A. Roebroeck, R. Galuske, E. Formisano, O. Chiry, H. Bratzke, I. Ronen, D.-S. Kim, and R. Goebel, "High-resolution diffusion tensor imaging and tractography of the human optic chiasm at 9.4 T," *NeuroImage*, vol. 39, pp. 157–168, 2008.

[7] K. Carlsson, P. Danielsson, R. Lenz, A. Liljeborg, and N. Åslund, "Three-dimensional microscopy using a confocal laser scanning microscope," *Optics Letter*, vol. 10, pp. 53–55, 1985.

[8] W. Denk, J. H. Strickler, and W. W. Webb, "Two-photon laser scanning fluorescence microscopy," *Science*, vol. 248, pp. 73–76, 1990.

[9] J. B. Pawley, *Handbook of Biological Confocal Microscopy*. New York: Springer, 2005.

[10] D. Mayerich, L. C. Abbott, and B. H. McCormick, "Knife-edge scanning microscopy for imaging and reconstruction of three-dimensional anatomical structures of the mouse brain," *Journal of Microscopy*, vol. 231, pp. 134–143, 2008.

[11] B. H. McCormick, "System and method for imaging an object," 2004, uSPTO patent #US 6,744,572 (for Knife-Edge Scanning; 13 claims).

[12] B. H. McCormick, Y. Choe, W. Koh, L. C. Abbott, J. Keyser, Z. Melek, P. Doddapaneni, and D. Mayerich, "Construction of anatomically correct models of mouse brain networks," *Neurocomputing*, vol. 58–60, pp. 379–386, 2004.

[13] A. Li, H. Gong, B. Zhang, Q. Wang, C. Yan, J. Wu, Q. Liu, S. Zeng, and Q. Luo, "Micro-optical sectioning tomography to obtain a high-resolution atlas of the mouse brain," *Science*, vol. 330, pp. 1404–1408, 2010, *See the E-Letter commentary by Mayerich et al.*

[14] K. Micheva and S. J. Smith, "Array tomography: A new tool for imaging the molecular architecture and ultrastructure of neural circuits," *Neuron*, vol. 55, pp. 25–36, 2007.

[15] P. S. Tsai, B. Friedman, A. I. Ifarraguerri, B. D. Thompson, V. Lev-Ram, C. B. Schaffer, Q. Xiong, R. Y. Tsien, J. A. Squier, and D. Kleinfeld, "All-optical histology using ultrashort laser pulses," *Neuron*, vol. 39, pp. 27–41, 2003.

[16] B. A. Wilt, L. D. Burns, E. T. W. Ho, K. K. Ghosh, E. A. Mukamel, and M. J. Schnitzer, "Advances in light microscopy for neuroscience," *Annual Reviews of Neuroscience*, vol. 32, pp. 435–506, 2009.

[17] W. Denk and H. Horstmann, "Serial block-face scanning electron microscopy to reconstruct three-dimensional tissue nanostructure," *PLoS Biology*, vol. 19, p. e329, 2004.

[18] K. Hayworth, "Automated creation and SEM imaging of Ultrathin Section Libraries: Tools for large volume neural circuit reconstruction," in *Society for Neuroscience Abstracts*. Washington, DC: Society for Neuroscience, 2008, program No. 504.4.

[19] J. A. Heymann, M. Hayles, I. Gestmann, L. A. Giannuzzi, B. Lich, and S. Subramaniam, "Site-specific 3D imaging of cells and tissues with a dual beam microscope," *Journal of Structural Biology*, vol. 155, pp. 63–73, 2006.

[20] B. H. McCormick, "The knife-edge scanning microscope," Department of Computer Science, Texas A&M University, Tech. Rep., 2003, http://research.cs.tamu.edu/bnl/.

[21] J. Kwon, D. Mayerich, Y. Choe, and B. H. McCormick, "Lateral sectioning for knife-edge scanning microscopy," in *Proceedings of the IEEE International Symposium on Biomedical Imaging*, 2008, pp. 1371–1374.

[22] J.-R. Kwon, "Acquisition and mining of the whole mouse brain microstructure," Ph.D. dissertation, Department of Computer Science, Texas A&M University, 2009.

[23] Y. Choe, D. Han, P.-S. Huang, J. Keyser, J. Kwon, D. Mayerich, and L. C. Abbott, "Complete submicrometer scans of mouse brain microstructure: Neurons and vasculatures," in *Neuroscience Meeting Planner, Chicago, IL: Society for Neuroscience*, 2009, program No. 389.10. Online.

[24] L. C. Abbott, "High-throughput imaging of whole small animal brains with the knife-edge scanning microscope," in *Neuroscience Meeting Planner, Washington, DC: Society for Neuroscience*, 2008, program No. 504.2.

[25] Y. Choe, L. C. Abbott, D. E. Miller, D. Han, H.-F. Yang, J. R. Chung, C. Sung, D. Mayerich, J. Kwon, K. Micheva, and S. J. Smith, "Multiscale imaging, analysis, and integration of mouse brain networks," in *Neuroscience Meeting Planner, San Diego, CA: Society for Neuroscience*, 2010, program No. 516.3. Online.

[26] D. C.-Y. Eng and Y. Choe, "Stereo pseudo 3D rendering for web-based display of scientific volumetric data," in *Proceedings of the IEEE/EG International Symposium on Volume Graphics*, 2008.

[27] S. Bovetti, Y.-C. Hsieh, P. Bovolin, I. Perroteau, T. Kazunori, and A. C. Puche, "Blood vessels form a scaffold for neuroblast migration in the adult olfactory bulb," *The Journal of Neuroscience*, vol. 27, pp. 5976–5980, 2007.

[28] Z. Melek, D. Mayerich, C. Yuksel, and J. Keyser, "Visualization of fibrous and thread-like data," *IEEE Transactions on Visualization and Computer Graphics*, vol. 12, no. 5, pp. 1165–1172, 2006.

[29] D. Mayerich, L. C. Abbott, and J. Keyser, "Visualization of cellular and microvessel relationship," *IEEE Transactions on Visualization and Computer Graphics (Proceedings of IEEE Visualization)*, vol. 14, pp. 1611–1618, 2008.

[30] D. Mayerich, J. Kwon, Y. Choe, L. Abbott, and J. Keyser, "Constructing high-resolution microvascular models," in *Proceedings of the 3rd International Workshop on Microscopic Image Analysis with Applications in Biology (MIAAB 2008)*, 2008, online.

[31] A. Can, H. Shen, J. N. Turner, H. L. Tanenbaum, and B. Roysam, "Rapid automated tracing and feature extraction from retinal fundus images using direct exploratory algorithms," *IEEE Transactions on Information Technology in Biomedicine*, vol. 3, pp. 125–138, 1999.

[32] D. Han, J. Keyser, and Y. Choe, "A local maximum intensity projection tracing of vasculature in Knife-Edge Scanning Microscope volume data," in *Proceedings of the IEEE International Symposium on Biomedical Imaging*, 2009, pp. 1259–1262.

[33] D. Han, H. Choi, C. Park, and Y. Choe, "Fast and accurate retinal vasculature tracing and kernel-isomap-based feature selection," in *Proceedings of the International Joint Conference on Neural Networks*. Piscataway, NJ: IEEE Press, 2009, pp. 1075–1082.

[34] K. A. Al-Kofahi, S. Lasek, D. H. Szarowski, C. J. Pace, G. Nagy, J. N. Turner, and B. Roysam, "Rapid automated three-dimensional tracing of neurons from confocal image stacks," *IEEE Transactions on Information Technology in Biomedicine*, vol. 6, pp. 171–187, 2002.

[35] H.-F. Yang and Y. Choe, "Cell tracking and segmentation in electron microscopy images using graph cuts," in *Proceedings of the IEEE International Symposium on Biomedical Imaging*, 2009, pp. 306–309.

[36] ——, "Electron microscopy image segmentation with estimated symmetric three-dimensional shape prior," in *Proceedings of the 6th International Symposium on Visual Computing*, 2010, in press.

[37] ——, "3D volume extraction of densely packed cells in EM data stack by forward and backward graph cuts," in *Proceedings of the 2009 IEEE Symposium on Computational Intelligence for Multimedia Signal and Vision Processing*, 2009, pp. 47–52.

[38] J. C. Fiala, "Reconstruct: A free editor for serial section microscopy," *Jounral of Microscopy*, vol. 218, pp. 52–61, 2005.

[39] J. R. Glaser and E. M. Glaser, "Neuron imaging with Neurolucida–A PC-based system for image combining microscopy," *Computerized Medical Imaging and Graphics*, vol. 14, pp. 307–317, 1990.

[40] MicroBrightField, Inc., "Neurolucida," http://www.mbfbioscience.com/neurolucida.

[41] V. Jain, J. F. Murray, F. Roth, S. Turaga, V. Zhigulin, K. L. Briggman, M. N. Helmstaedter, W. Denk, and H. S. Seung, "Supervised learning of image restoration with convolutional networks," in *IEEE 11th International Conference on Computer Vision (ICCV 2007)*, 2007, pp. 1–8.

[42] D. Mayerich, J. Kwon, A. Panchal, J. Keyser, and Y. Choe, "Fast cell detection in high-throughput imagery using gpu-accelerated machine learning," in *Proceedings of the IEEE International Symposium on Biomedical Imaging*, 2011, in press.

[43] S. J. Warfield, K. H. Zou, and W. M. Wells, "Validation of image segmentation and expert quality with expectation-minimization algorithm," in *Lecture Notes In Computer Science, Vol. 2488; Proceedings of the 5th International Conference on Medical Image Computing and Computer-Assisted Intervention*, 2002, pp. 298–306.

[44] D. Han, "Rapid 3D tracing of the mouse brain neurovasculature with local maximum intensity projection and moving windows," Ph.D. dissertation, Department of Computer Science, Texas A&M University, 2009.

[45] J. G. White, E. Southgate, J. N. Thomson, and S. Brenner, "The structure of the nervous system of the nematode caenorhabditis elegans," *Philosophical Transactions of the Royal Society of London B*, vol. 314, pp. 1–340, 1986.

[46] O. Sporns and G. Tononi, "Classes of network connectivity and dynamics," *Complexity*, vol. 7, pp. 28–38, 2002.

[47] A.-L. Barabasi, *Linked: The New Science of Networks*. Cambridge, MA: Perseus Publishing, 2002.

[48] O. Sporns, "Graph theory methods for the analysis of neural connectivity patterns," in *Neuroscience Databases: A Practical Guide*, R. Kötter, Ed. Boston, MA: Kluwer Publishers, 2002.

[49] R. Milo, S. Sen-Orr, S. Itzkovitz, N. Kashtan, D. Chklovskii, and U. Alon, "Network motifs: Simple building blocks of complex networks," *Science*, vol. 298, pp. 824–827, 2002.

[50] G. M. Shepherd, *The Synaptic Organization of the Brain*, 5th ed. Oxford, UK; New York: Oxford University Press, 2004.

[51] A. Thiel, H. Schwegler, and C. W. Eurich, "Complex dynamics is abolished in delayed recurrent systems with distributed feedback times," *Complexity*, vol. 8, pp. 102–108, 2003.

[52] O. Sporns, G. Tononi, and G. M. Edelman, "Connectivity and complexity: The relationship between neuroanatomy and brain dynamics." *Neural Networks*, vol. 13, pp. 909–922, 2000.

[53] N. Kalisman, G. Silberberg, and H. Markram, "Deriving physical connectivity from neuronal morphology," *Biological Cybernetics*, vol. 88, pp. 210–218, 2003.

[54] M. Toledo-Rodriguez, B. Blumenfeld, C. Wu, J. Luo, B. Attali, P. Goodman, and H. Markram, "Correlation maps allow neuronal electrical properties to be predicted from single-cell gene expression profiles in rat neocortex," *Cerebral Cortex*, vol. 14, pp. 1310–1327, 2004.

[55] E. S. Lein et al., "Genome-wide atlas of gene expression in the adult mouse brain," *Nature*, vol. 445, pp. 168–176, 2007.

[56] H. Markram, "The blue brain project," *Nature Reviews Neuroscience*, vol. 7, pp. 153–160, 2006.

[57] G. A. Ascoli, D. E. Donohue, and M. Halavi, "NeuroMorpho.Org: A central resource for neuronal morphologies," *Journal of Neuroscience*, vol. 27, pp. 9247–9251, 2007.

[58] B. W. Mel, "Information processing in dendritic trees," *Neural Computation*, vol. 6, pp. 1031–1085, 1994.

[59] A. Polsky, B. W. Mel, and J. Schiller, "Computational subunits in thin dendrites of pyramidal cells," *Nature Neuroscience*, vol. 7, pp. 821–827, 2004.

[60] P. Dayan and L. F. Abbott, *Theoretical Neuroscience*. Cambridge, MA: MIT Press, 2001.

[61] M. L. Hines and N. T. Carnevale, "The NEURON simulation environment," *Neural Computation*, vol. 9, pp. 1179–1209, 1997.

[62] J. M. Bower and D. Beeman, *The Book of GENESIS: Exploring Realistic Neural Models with the GEneral NEural SImulation System*. Santa Clara, CA: Telos, 1998.

[63] P. Gleeson, V. Steuber, and R. Silver, "NeuroConstruct: A tool for modeling networks of neurons in 3D space," *Neuron*, vol. 54, pp. 219–235, 2007.

[64] R. A. Koene, B. Tijms, P. van Hees, F. Postma, A. de Ridder, G. J. A. Ramakers, J. van Pelt, and A. van Ooyen, "NETMORPH: A framework for the stochastic generation of large scale neuronal networks with realistic neuron morphologies," *Neuroinformatics*, vol. 7, pp. 1539–2791, 2009.

[65] R. A. Koene, "Large scale high resolution network generation: Producing known validation sets for serial reconstruction methods that use histological images of neural tissue," in *International Conference on Complex Systems*, 2007, [Presentation].

[66] G. Ascoli, J. Krichmar, R. Scorcioni, S. Nasuto, and S. Senft, "Computer generation and quantitative morphometric analysis of virtual neurons," *Anatomical Embryology*, vol. 204, pp. 283–301, 2001.

[67] J. P. Eberhard, A. Wanner, and G. Wittum, "NeuGen: A tool for the generation of realistic morphology of cortical neurons and neural networks," *Neurocomputing*, vol. 70, pp. 327–342, 2006.

[68] S. Druckmann, T. K. Berger, S. Hill, F. Schürmann, H. Markram, and I. Segev, "Evaluating automated parameter constraining procedures of neuron models by experimental and surrogate data," *Biological Cybernetics*, vol. 99, pp. 371–379, 2008.

[69] E. M. Izhikevich and G. M. Edelman, "Large-scale model of mammalian thalamocortical systems," *Proceedings of the National Academy of Sciences, USA*, vol. 105, pp. 3593–3598, 2008.

[70] Y. Choe, L. C. Abbott, G. Ponte, J. Keyser, J. Kwon, D. Mayerich, D. Miller, D. Han, A. M. Grimaldi, G. Fiorito, D. B. Edelman, and J. L. McKinstry, "Charting out the octopus connectome at submicron resolution using the knife-edge scanning microscope," *BMC Neuroscience*, vol. 11(Suppl 1), p. P136, 2010, nineteenth Annual Computational Neuroscience Meeting: CNS*2010.

[71] J. Pearl, "Reasoning with cause and effect," *AI Magazine*, vol. 23, pp. 95–111, 2001.

[72] Y. Choe, H.-F. Yang, and D. C.-Y. Eng, "Autonomous learning of the semantics of internal sensory states based on motor exploration," *International Journal of Humanoid Robotics*, vol. 4, pp. 211–243, 2007.

[73] J. R. Chung, J. Kwon, and Y. Choe, "Evolution of recollection and prediction in neural networks," in *Proceedings of the International Joint Conference on Neural Networks*. Piscataway, NJ: IEEE Press, 2009, pp. 571–577.

[74] J. Kwon and Y. Choe, "Facilitating neural dynamics for delay compensation: A road to predictive neural dynamics?" *Neural Networks*, vol. 22, pp. 267–276, 2009.